

# Effects of cyclic loading on soil-geogrid interaction characteristics

*Fernanda B. Ferreira<sup>#</sup>, Castorina S. Vieira, Maria de Lurdes Lopes, and Pedro G. Ferreira*

*CONSTRUCT, Faculty of Engineering, University of Porto, R. Dr. Roberto Frias, 4200-465 Porto, Portugal*

*<sup>#</sup>Corresponding author: [fbf@fe.up.pt](mailto:fbf@fe.up.pt)*

## ABSTRACT

The benefits of geosynthetic-reinforced soil systems over conventional earth-retaining structures are now well established. These reinforced systems are often subjected not only to static loads, but also to seismic and/or traffic loads, in which case the effects of repeated loading on soil-geosynthetic interaction characteristics should be properly considered. This study investigates the behaviour of a geogrid typically used for soil reinforcement under cyclic pullout loading through load-controlled laboratory pullout tests. To examine the influence of cyclic loading amplitude, number of cycles and static pullout force acting on the geogrid at the onset of cyclic loading, distinct loading patterns are considered. A well-graded residual soil from granite is used as backfill material. A comparison between the cyclic and monotonic pullout response of the reinforcement is then established in order to identify any potential strength loss attributed to cyclic loading. The experimental results show that the ultimate pullout resistance of the geogrid embedded in medium dense residual soil from granite may be adversely affected by cyclic loading. The cumulative cyclic displacements of the reinforcement are more pronounced during the initial loading cycles, but tend to stabilize with the increasing number of cycles when the soil is densely compacted. In the presence of dense soil, the cyclic strains of the geogrid specimen are particularly significant at the front section and almost negligible towards the back end.

**Keywords:** pullout test; soil-geogrid interaction; cyclic and post-cyclic interface response; residual soil from granite.

## 1. Introduction

Geosynthetic-reinforced soil systems, such as retaining walls, embankments and bridge abutments, have increasingly been used over the past few decades and have proven to offer a sustainable alternative to more traditional earth retaining structures (e.g., reinforced concrete walls). Among the advantages of these reinforced soil systems are the cost-effectiveness, lower construction time, flexibility, ductility, and the potential use of locally available low-quality soils or recycled waste materials, which would otherwise be disposed of in landfills (Ferreira et al. 2020a, 2023). When these structures are constructed in seismically active regions or used in transport infrastructure projects, the effects of repeated loading on the structure performance should be carefully taken into account (Min et al. 1995, Raju and Fannin 1998, Moraci et al. 2009, 2012, Razzazan et al. 2018, Cardile et al. 2019, Ferreira et al. 2020b, Vieira et al. 2020, Watanabe et al. 2022). In particular, the pullout resistance of the reinforcement under cyclic loading conditions is an important parameter for the internal stability analysis and design of these geosynthetic-reinforced soil systems.

Residual soils derive from the mechanical and chemical weathering of the underlying parent rock. They can be found in many parts of the world and are widely used in construction, but the knowledge about their mechanical behaviour is not as extensive as that for transported soils. Residual soils from granite are predominant in Northern Portugal and most of the

buildings and structures in this region are founded on these soils. The behaviour of these residual soils is often significantly different from that of transported soils with similar particle size distributions and densities (Viana da Fonseca et al. 1997).

The main purpose of this study is to assess the effects of cyclic loading on the interface behaviour between a locally available residual soil from granite and a uniaxial geogrid typically used for soil reinforcement applications under pullout loading conditions. The results of large-scale pullout tests involving cyclic loading are presented and compared with those of monotonic tests used as the benchmark. The strain and displacement behaviour of the geogrid when subjected to cyclic loading histories with different characteristics is also evaluated and discussed.

## 2. Experimental study

### 2.1. Residual soil from granite

The soil used in this experimental study was a residual soil from granite with the particle size distribution curve shown in Fig. 1. According to the Unified Soil Classification System, this soil is classified as SW-SM (well-graded sand with silt and gravel). The dry density-moisture content relationship was assessed using the Modified Proctor test (CEN 2010). The maximum dry density and the optimum moisture content were determined as 18.9 kN/m<sup>3</sup> and 11.5%, respectively. The internal shear strength of the soil was characterized by large-scale direct shear tests (Ferreira et al. 2015).

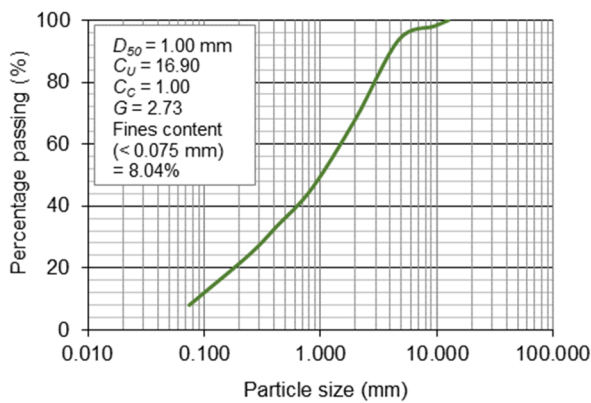


**Figure 1.** Soil gradation.

## 2.2. Geogrid

The geogrid employed in this research (Fig. 2) was an extruded uniaxial geogrid manufactured from high-density polyethylene (HDPE), with a mean grid size of about 22 mm × 235 mm. The tensile load-strain behaviour of the geogrid was evaluated using wide-width tensile tests according to EN ISO 10319: 2015 (CEN 2015). As shown in Fig. 3, the mean values of the tensile strength ( $T_{max}$ ), elongation at maximum load ( $\epsilon_{Tmax}$ ), and secant stiffness at 5% strain ( $J_{5\%}$ ) of five specimens tested under repeatability conditions were 52.2 kN/m, 12.4%, and 509.8 kN/m, respectively.

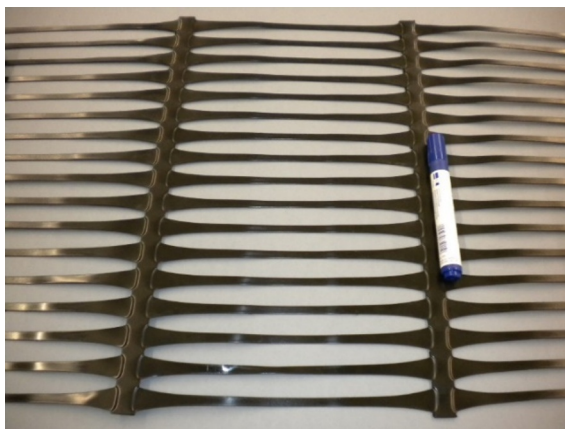


**Figure 2.** Visual aspect of the geogrid.

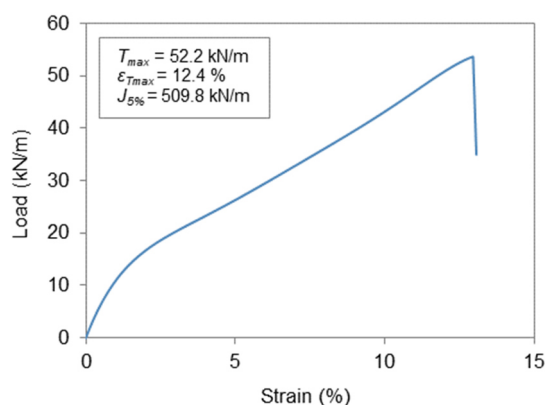


**Figure 3.** Mean load-strain curve of the geogrid (machine direction).

## 2.3. Apparatus and test method

The pullout tests reported here were carried out using large-scale pullout test equipment (1.53 m long × 1.00 m wide × 0.80 m deep) driven by a closed-loop servo-hydraulic control system. Further details on this test facility and associated instrumentation system can be found elsewhere (Lopes and Ladeira 1996a, 1996b, Ferreira et al. 2016, 2020b, Vieira et al. 2020).

The residual soil from granite was compacted in the pullout box in the air-dried moisture condition in several 0.15 m thick layers up to a total height of 0.60 m. Once the first two layers were compacted to the desired relative density, the geogrid specimen (0.33 m wide by 1.00 m long) was clamped and positioned inside the pullout box over the compacted soil. The upper soil layers were then placed and compacted following identical procedures to those used for the bottom layers. The prescribed vertical pressure was imposed through a wooden plate loaded by a set of hydraulic jacks and the pullout load was then applied to the geogrid specimen.

The pullout tests to evaluate the effects of cyclic loading on soil-geogrid interaction characteristics were performed under load-controlled conditions, using a multistage procedure. After an initial monotonic loading stage, where the pullout force was applied to the geosynthetic under a uniform rate of load application (0.7 kN/m/min) up to the pullout force level  $P_L$ , a series of loading cycles with a given amplitude ( $A$ ) and frequency ( $f$ ) was applied. Upon completion of the prescribed number of cycles ( $N$ ), a monotonic loading (identical to that of the first stage) was imposed until the end of the test. It should be noted that the values of amplitude and pullout force level from which the cyclic loading was applied were defined on the basis of the ultimate pullout resistance ( $P_R$ ) obtained from monotonic pullout tests. These tests were also carried out under load-controlled mode, using a uniform rate of load application (0.7 kN/m/min) until pullout or failure of the geogrid was achieved.

## 2.4. Test programme

To investigate the influence of the load level applied on the reinforcement when the cyclic loading takes place, different  $P_L$  values of  $0.25P_R$ ,  $0.50P_R$  and  $0.65P_R$  were considered. These values were selected to mimic three distinct levels of static pullout force already acting on the geogrid when the cyclic load is applied. Indeed, in the field, geosynthetics can be subjected to varying levels of static pullout force induced by the self-weight of the structure and any external dead loads.

Furthermore, to simulate different cyclic loading patterns, such as those experienced under actual field conditions, the amplitude of cyclic loading applied in this study ranged from  $0.15P_R$  to  $0.40P_R$ , whereas the number of loading cycles varied between 40 and 120.

In addition, the compaction conditions of the residual soil from granite were changed so that the aforementioned factors could be investigated in the presence of both dense (i.e.  $\gamma_d = 17.3 \text{ kN/m}^3$ ,  $I_D = 85\%$ ) and medium dense (i.e.  $\gamma_d = 15.3 \text{ kN/m}^3$ ,  $I_D = 50\%$ ) soil. Even though geosynthetic-reinforced soil systems

typically involve densely compacted backfills to ensure adequate performance throughout the design lifetime, this study aimed at characterizing the influence of soil placement density on the geogrid pullout response.

Monotonic load-controlled pullout tests were also performed with the geogrid embedded in medium dense and dense soil (i.e. under compaction conditions identical to those adopted in the cyclic tests) and used as the benchmark.

All of the aforementioned tests were conducted under a constant vertical pressure of 25 kPa, resembling relatively low depths, where the pullout failure mechanism is most likely to occur in reinforced soil systems, such as walls and slopes.

### 3. Results and discussion

#### 3.1. Pullout tests under monotonic loading conditions

As mentioned earlier, the geogrid pullout response under monotonic loading was evaluated by load-controlled pullout tests using a constant load increment rate of 0.7 kN/m/min up to failure. These tests were used as the benchmark to investigate the effects of cyclic loading on the mechanical behaviour at the soil-geogrid interface.

Fig. 4 presents the results from monotonic tests for different conditions of soil density. As expected, the geogrid embedded in denser soil ( $I_D = 85\%$ ) exhibited a stiffer response and a well-defined peak of strength was obtained at a frontal displacement of about 70 mm (Fig. 4a). The ultimate pullout resistance of the geogrid in contact with dense soil (39.9 kN/m) significantly exceeded that achieved when the soil was tested under medium dense conditions (29.3 kN/m).

Furthermore, the increase in soil density affected the mode of failure at the interface. While in the presence of medium dense soil the failure was attributed to the geogrid sliding (pullout failure), a different type of failure (reinforcement breakage or tensile failure) occurred when the geogrid was placed in denser soil. This explains the fast reduction in the pullout force beyond the peak value.

The displacements measured throughout the length of the geogrid at the ultimate pullout resistance are illustrated in Fig. 4(b). For  $I_D = 85\%$ , the displacement at the back end of the reinforcement was almost negligible, and hence the displacements measured over the length of the reinforcement were mainly attributed to elongation. In contrast, for  $I_D = 50\%$ , the displacement at the back end of the geogrid was significantly higher (35.5 mm), clearly indicating that the reinforcement sliding was the mechanism leading to interface failure.

It is interesting to note that the maximum pullout force reached in the test performed with dense soil (39.9 kN/m), in which the failure was caused by the reinforcement breakage, was significantly lower than the average tensile strength of 52.2 kN/m<sup>3</sup> obtained from in-isolation wide-width tensile tests (Fig. 3). Besides, the strain at failure in the tensile tests (Fig. 3) was about a half of that experienced by the geogrid in dense soil (Fig. 4b). In the pullout test, large deformations were produced

over the front sections of the geogrid, implying that the greatest portion of the applied load was mobilized throughout the front half of the reinforcement and only a small portion was transferred to the rear sections. This fact, associated with the high level of tension mobilized against the first confined transverse member of the reinforcement (due to the passive resistance mechanism) induced the premature failure of the geogrid specimen (i.e. the rupture occurred under a pullout force considerably lower than the respective in-isolation tensile strength). A similar conclusion was also reported in a previous related study (Ferreira et al. 2016).

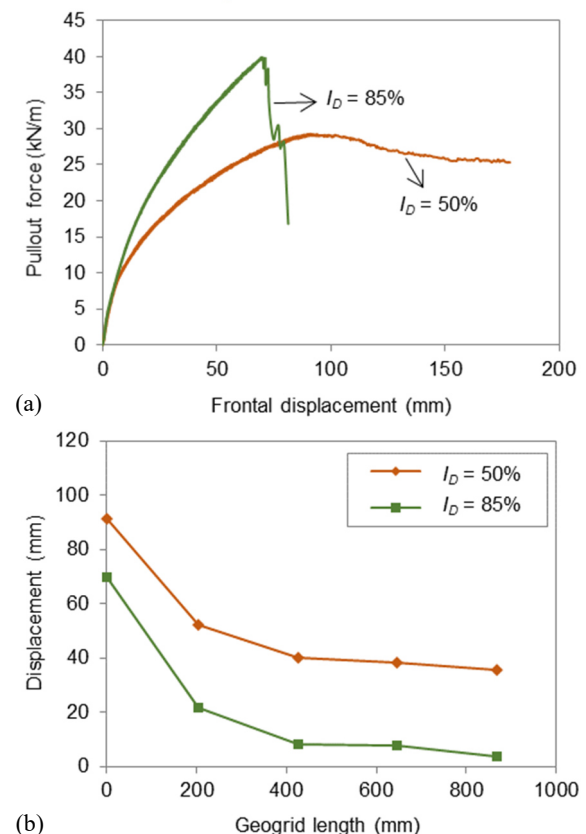


**Figure 4.** Pullout test results under monotonic loading: (a) pullout force-frontend displacement relationship; (b) displacements over the geogrid length at the ultimate pullout resistance.

#### 3.2. Pullout tests under cyclic loading conditions

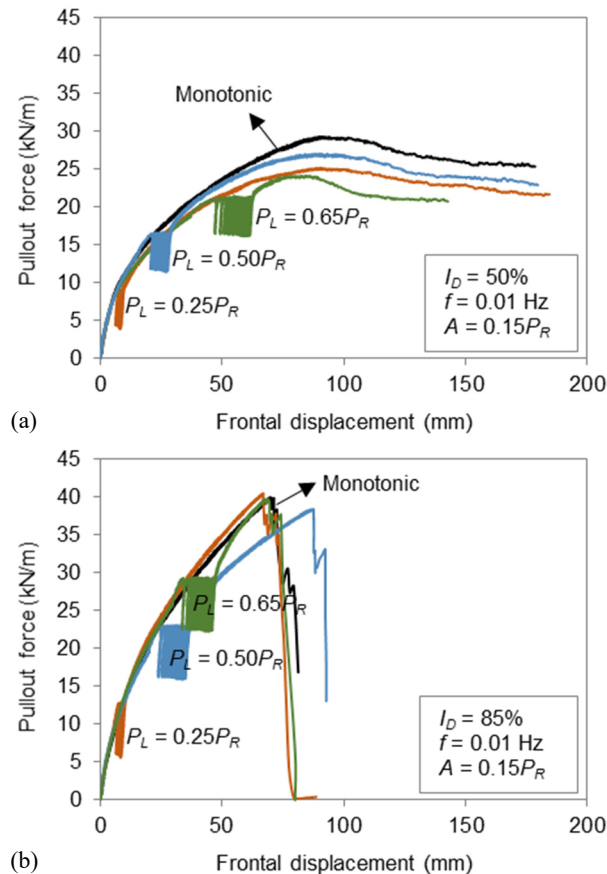
A series of pullout tests was carried out to analyse the influence of cyclic loading on soil-geogrid interaction and to understand to which extent several factors, including the pullout force applied on the reinforcement prior to the cyclic loading stage ( $P_L$ ), the cyclic loading amplitude ( $A$ ) and the number of cycles ( $N$ ) could affect the geogrid pullout response.

Fig. 5 illustrates the pullout force-frontend displacement relationship from three pullout tests in which  $P_L$  values of  $0.25P_R$ ,  $0.50P_R$  and  $0.65P_R$  were considered. Figs. 5(a) and 5(b) are associated with medium dense and dense soil, respectively. The corresponding monotonic curves are superimposed in these figures for comparison purposes.

Fig. 5(a) shows that, irrespective of the  $P_L$  value, the ultimate pullout resistance of the geogrid decreased in

comparison to that mobilized under monotonic loading conditions. The maximum reduction (about 17.7%) was obtained for  $P_L = 0.65P_R$  (the highest  $P_L$  value adopted here). However, in the presence of denser soil (Fig. 5b) the ultimate pullout resistance was not significantly affected by the  $P_L$  value. This is possibly related to the fact that the failure was caused by the reinforcement internal rupture, suggesting that the confined tensile strength of the geogrid was not affected by the cyclic loading histories.

The evolution of displacements over  $N = 40$  cycles at the front and back ends of the geogrid specimen for distinct  $P_L$  values is depicted in Fig. 6. Note that these displacements were recorded at the maximum force applied during a given loading cycle. It can be seen that the rate of displacement accumulation was more pronounced during the initial cycles. In addition, the higher the  $P_L$  value, the larger the cumulative displacement measured during cyclic loading. The geogrid front displacements consistently exceed those of the free end, which is attributed to the reinforcement elongation induced by cyclic loading. The displacements recorded at the back end of the reinforcement in the presence of medium dense soil (Fig. 6a) clearly exceeded those obtained with dense soil (Fig. 6b) under otherwise identical test conditions.



**Figure 5.** Influence of  $P_L$  on the pullout force-frontal displacement relationship: (a) medium dense soil; (b) dense soil.

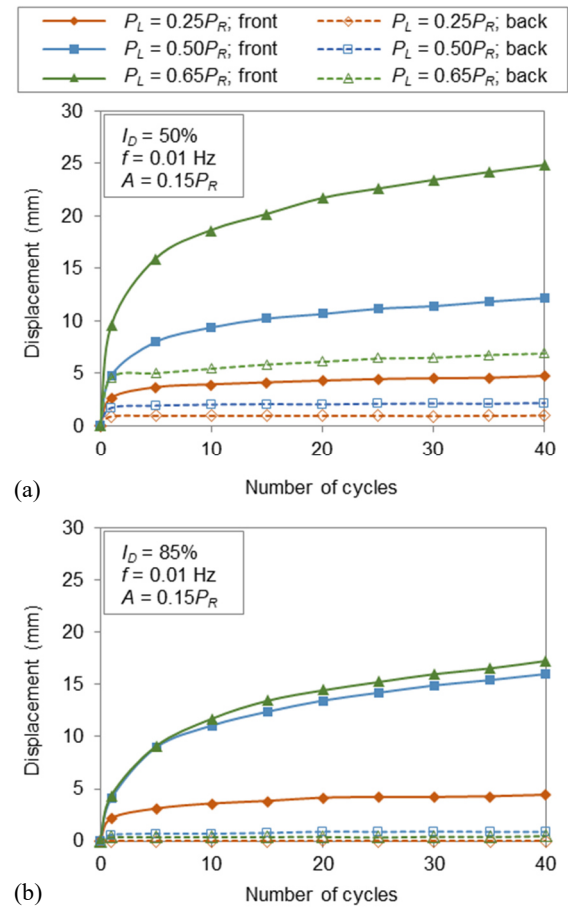


**Figure 6.** Influence of  $P_L$  on the displacements induced by cyclic loading at the front and back geogrid ends: (a) medium dense soil; (b) dense soil.

The displacements recorded over the length of the reinforcement at the onset of cyclic loading (pre-cyclic) and after cyclic loading, when the pullout force returned to the initial value  $P_L$  (post-cyclic), are plotted in Fig. 7. As expected, the increase in  $P_L$  generally resulted in an increase in the pre-cyclic displacements along the specimen. However, for  $I_D = 85\%$  (Fig. 7b), only the front section of the geogrid underwent additional deformation when the  $P_L$  value increased from 0.50 to  $0.65P_R$ . Fig. 7(a) also shows that when the soil was in medium dense state, the increase in  $P_L$  value led to higher displacements and strains over the geogrid length during cyclic loading. In contrast, when the soil was densely compacted (Fig. 7b), the increase in  $P_L$  resulted essentially in higher strains over the geogrid length (i.e. no significant sliding occurred along the interface).

To examine the effect of amplitude ( $A$ ) on soil-geogrid interaction under cyclic and post-cyclic pullout loading, two values of  $A$  were adopted, specifically  $0.15P_R$  and  $0.40P_R$ . Fig. 8(a) presents the pullout force-frontal displacement curves obtained from tests conducted using medium dense soil ( $I_D = 50\%$ ) and varying  $A$  values. Figs. 8(b) and 8(c) show the cumulative displacements resulting from cyclic loading at the front and back ends of the reinforcement, as well as the pre- and post-cyclic displacements over the reinforcement length, respectively.



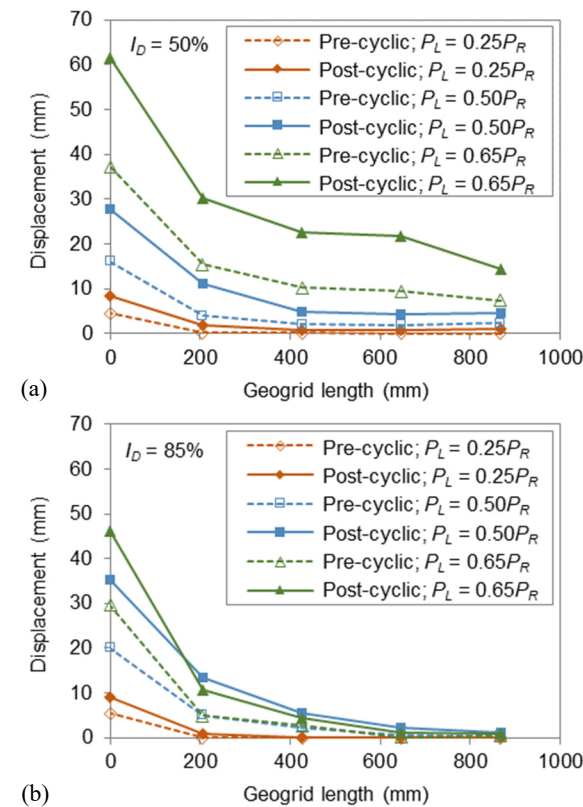


**Figure 7.** Influence of  $P_L$  on the displacements measured over the geogrid length before and after cyclic loading: (a) medium dense soil; (b) dense soil.

It is noteworthy that the increase in  $A$  in these tests did not produce any reduction in the ultimate pullout resistance mobilized during the post-cyclic stage. In fact, for  $A = 0.40P_R$  the ultimate pullout resistance was identical to that reached in the monotonic test, and exceeded that obtained under the lower  $A$  value. The frontal displacement at which the maximum pullout resistance was mobilized was barely affected by cyclic loading, regardless of amplitude (Fig. 8a).

As Fig. 8(b) shows, when the amplitude of cyclic loading increased, both the front and back ends of the geogrid experienced significantly higher displacements over the number of cycles. For instance, after 40 cycles, the cumulative frontal displacement under  $A = 0.40P_R$  was 35.3 mm, whereas a significantly lower cumulative value (12.2 mm) was attained under  $A = 0.15P_R$ .

The displacement profiles illustrated in Fig. 8(c) indicate that, as expected, the pre-cyclic displacements of the geogrid were nearly coincident for both  $A$  values, since they were taken at the onset of cyclic loading in two tests performed under the same experimental conditions (except for the  $A$  value). However, the post-cyclic displacements over the whole reinforcement length were significantly larger under the higher  $A$  value, clearly showing that the loading amplitude plays a significant role as far as the cyclic displacements along the geogrid are concerned. Moreover, the deformation of the geogrid induced by cyclic loading was particularly significant over the front half of its length. Indeed, the strains at the back half of the reinforcement were rather small for  $A = 0.40P_R$  and negligible for  $A = 0.15P_R$  (Fig. 8c).

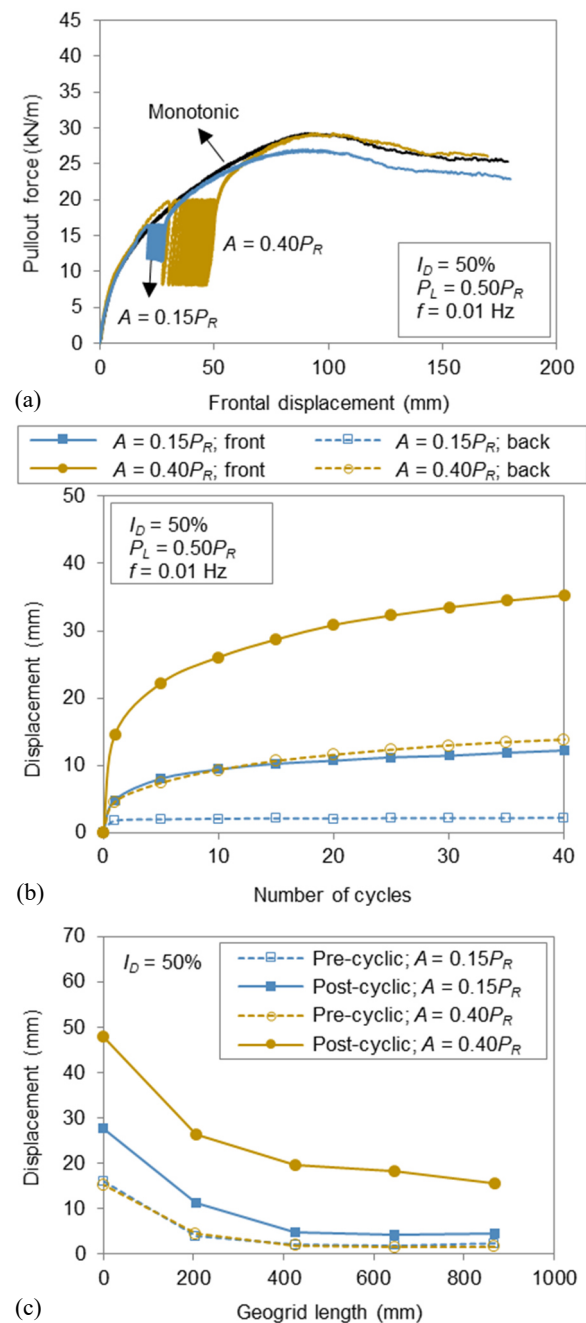


**Figure 8.** Influence of  $A$  on soil-geogrid interaction: (a) pullout force-frontal displacement relationship; (b) displacements induced by cyclic loading at the front and back geogrid ends; (c) displacements over the geogrid length before and after cyclic loading.

The number of loading cycles imposed at the soil-geosynthetic interface is another factor susceptible to affect the interface behaviour and the long-term stability of the reinforced soil structure. In order to gain further insight into the influence of the number of cycles ( $N$ ), two  $N$  values were adopted in this study: 40 and 120.

The evolution of the pullout force with the frontal geogrid displacement obtained from tests in which the number of cycles was changed is shown in Figs. 9(a) and 9(b), corresponding to medium dense and dense soil, respectively. Fig. 10 illustrates the evolution of geogrid displacements induced by cyclic loading in the tests performed with  $N = 120$  cycles.

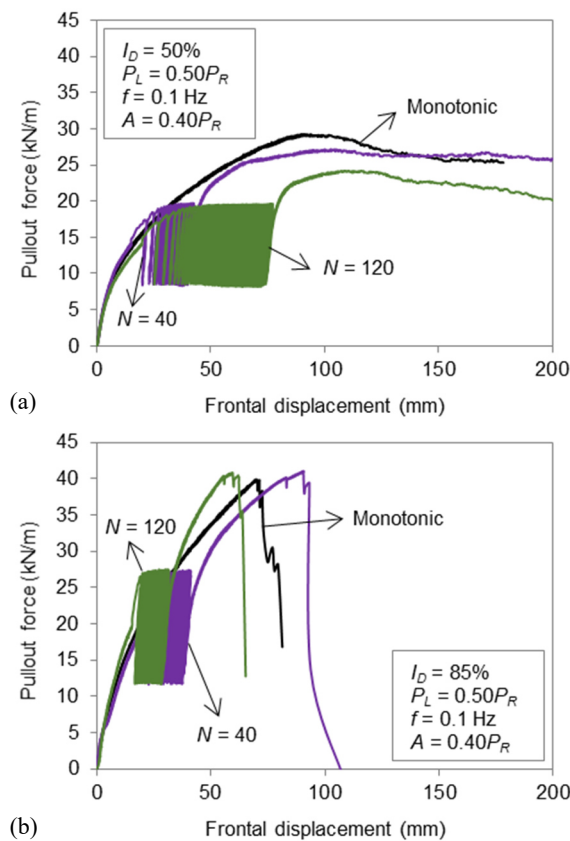


**Figure 9.** Influence of  $N$  on the pullout force-frontal displacement relationship: (a) medium dense soil; (b) dense soil.

It can be concluded that the effect of the number of cycles on the ultimate pullout resistance was quite different for distinct conditions of soil density. While for  $I_D = 50\%$  the ultimate pullout resistance of the reinforcement reduced considerably due to an increase in the number of cycles (Fig. 9a), for  $I_D = 85\%$  the peak load capacity remained nearly unchanged (Fig. 9b). In comparison with the monotonic test, the ultimate pullout resistance of the geogrid in medium dense soil decreased 7.1% and 17.3% for  $N = 40$  and  $N = 120$  cycles, respectively (Fig. 9a). On the other hand, in the presence of dense soil, the geogrid exhibited a stiffer response after being subjected to a larger number of loading cycles, with the maximum pullout force being reached at a frontal displacement that was lower than that observed in the comparable monotonic test (Fig. 9b).

As shown in Fig. 10(a), the cumulative displacements induced at the geogrid ends over 120 loading cycles were significantly larger for  $I_D = 50\%$ . Regardless of soil density, the rate of displacement accumulation was more pronounced during the first 20 cycles. However, for  $I_D = 50\%$  the displacements increased continuously at an almost constant rate after the first 20 cycles and until the end of the cyclic stage, denoting unstable interface response. In contrast, for  $I_D = 85\%$  the incremental displacements after the initial 20 cycles were not significant, indicating that the interface was relatively stable.

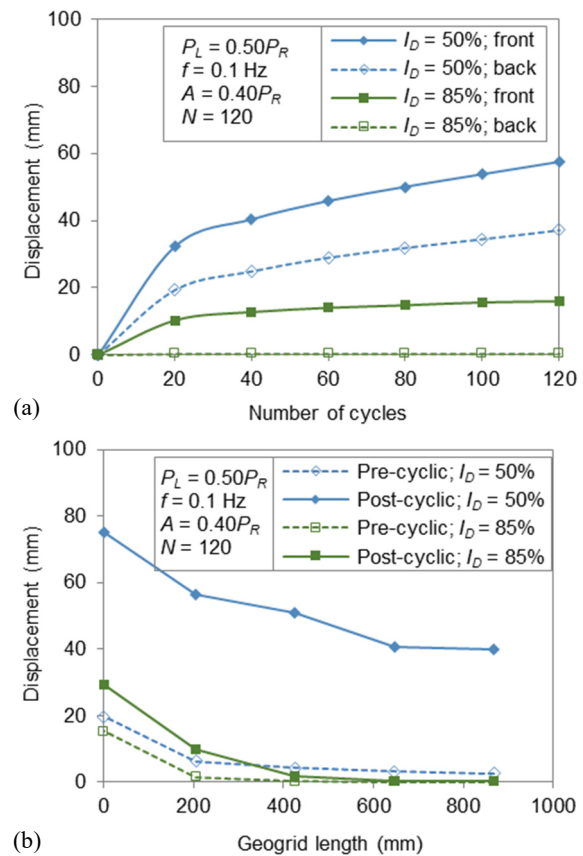


**Figure 10.** Evolution of geogrid displacements for  $N = 120$ : (a) displacements induced by cyclic loading at the front and back geogrid ends; (b) displacements over the geogrid length before and after cyclic loading.

Fig. 10(b) confirms that the reinforcement sliding resulting from cyclic loading (i.e. 120 cycles) may be exacerbated when the soil is poorly compacted ( $I_D = 50\%$ ). For  $I_D = 85\%$ , only geogrid strains were observed and no sliding occurred in these tests, despite the large number of cycles imposed at the interface. From the presented results, it becomes apparent that the effective compaction of the backfill material is a decisive factor contributing to enhanced stability of the soil-geogrid interface, and hence of the geosynthetic-reinforced soil system when subjected to repeated loading and unloading cycles.

## 4. Conclusions

This paper reported the results of large-scale load-controlled pullout tests carried out to investigate the effects of cyclic loading on soil-geogrid interaction characteristics. The main conclusions from this laboratory study are summarized below.

- Under monotonic loading conditions, the ultimate pullout resistance of the geogrid embedded in dense soil (39.9 kN/m) significantly exceeded that reached when the soil was in medium dense state (29.3 kN/m). For densely compacted soil, the geogrid displacements recorded at the ultimate pullout load were mainly attributed to elongation, whereas

significant sliding occurred under lower density conditions.

- When the soil was poorly compacted, the ultimate pullout resistance of the geogrid was detrimentally affected by cyclic loading (i.e. decreased by up to 18%). However, in the presence of dense soil, the geogrid post-cyclic pullout resistance remained similar to that reached in the corresponding monotonic test.
- The higher the pullout force applied on the reinforcement at the onset of the cyclic loading stage, the larger the cumulative displacements induced by cyclic loading at the loaded end, irrespective of soil density.
- The cyclic loading amplitude plays a significant role concerning the cyclic displacements mobilized along the geogrid length. When the amplitude increased, the geogrid experienced significantly higher displacements over the number of cycles.
- In the presence of medium dense soil, the increase in the number of cycles (from 40 to 120) led to a significant reduction in the ultimate pullout resistance of the geogrid. In addition, the rate of accumulation of geogrid displacements observed during cyclic loading denoted unstable interface response.
- For densely compacted soil, the increase in the number of cycles did not affect the peak pullout resistance of the reinforcement. Furthermore, only geogrid strains were observed during the cyclic loading stage and no significant sliding occurred, even after a large number of cycles ( $N = 120$ ).

## Acknowledgements

The first author wishes to acknowledge Grant No. 2021.03625.CEECIND from the Stimulus of Scientific Employment, Individual Support (CEEICIND) – 4th Edition provided by Fundação para a Ciência e Tecnologia (FCT). This work was financially supported by: Base Funding—UIDB/04708/2020 of the CONSTRUCT—Instituto de I&D em Estruturas e Construções—funded by national funds through the FCT/MCTES (PIDDAC).

## References

- Cardile, G., M. Pisano, and N. Moraci. "The influence of a cyclic loading history on soil-geogrid interaction under pullout condition", *Geotext Geomembr*, 47(4), pp. 552-565, 2019, <https://doi.org/10.1016/j.geotexmem.2019.01.012>
- CEN "EN 13286-2:2010. Unbound and hydraulically bound mixtures - Part 2: Test methods for laboratory reference density and water content - Proctor compaction", CEN, Brussels, Belgium, 2010.
- CEN "EN ISO 10319:2015. Geosynthetics - Wide-width tensile test", CEN, Brussels, Belgium, 2015.
- Ferreira, F. B., C. S. Vieira, and M. L. Lopes. "Direct shear behaviour of residual soil-geosynthetic interfaces - influence of soil moisture content, soil density and geosynthetic type", *Geosynth Int*, 22(3), pp. 257-272, 2015, <https://doi.org/10.1680/jgein.15.00011>
- Ferreira, F. B., C. S. Vieira, and M. L. Lopes. "Pullout behavior of different geosynthetics - Influence of soil density and moisture content", *Front Built Environ*, 6(12), pp. 1-13, 2020a, <https://doi.org/10.3389/fbuil.2020.00012>
- Ferreira, F. B., C. S. Vieira, M. L. Lopes, and D. M. Carlos. "Experimental investigation on the pullout behaviour of geosynthetics embedded in a granite residual soil", *Eur J Environ Civ Eng*, 20(9), pp. 1147-1180, 2016, <https://doi.org/10.1080/19648189.2015.1090927>
- Ferreira, F. B., C. S. Vieira, M. L. Lopes, and P. G. Ferreira. "HDPE geogrid-residual soil interaction under monotonic and cyclic pullout loading", *Geosynth Int*, 27(1), pp. 79-96, 2020b, <https://doi.org/10.1680/jgein.19.00057>
- Ferreira, F. B., C. S. Vieira, P. M. Pereira, and M. L. Lopes. "Recycled construction and demolition waste as backfill material for geosynthetic-reinforced structures", In: *Sustainable Civil Engineering: Principles and Applications*, 1st ed., CRC Press, Taylor & Francis Group, Boca Raton, Florida, USA, 2023, pp. 1-27.
- Lopes, M. L., and M. Ladeira. "Role of specimen geometry, soil height and sleeve length on the pull-out behaviour of geogrids", *Geosynth Int*, 3(6), pp. 701-719, 1996a, <https://doi.org/10.1680/jgein.3.0081>
- Lopes, M. L., and M. Ladeira. "Influence of the confinement, soil density and displacement rate on soil-geogrid interaction", *Geotext Geomembr*, 14(10), pp. 543-554, 1996b, [https://doi.org/10.1016/S0266-1144\(97\)83184-6](https://doi.org/10.1016/S0266-1144(97)83184-6)
- Min, Y., D. Leshchinsky, H. Ling, and V. Kaliakin. "Effects of sustained and repeated tensile loads on geogrid embedded in sand", *Geotech Test J*, 18(2), pp. 204-225, 1995, <https://doi.org/10.1520/GTJ10322J>
- Moraci, N., and G. Cardile. "Influence of cyclic tensile loading on pullout resistance of geogrids embedded in a compacted granular soil", *Geotext Geomembr*, 27(6), pp. 475-487, 2009, <https://doi.org/10.1016/j.geotexmem.2009.09.019>
- Moraci, N., and G. Cardile. "Deformative behaviour of different geogrids embedded in a granular soil under monotonic and cyclic pullout loads", *Geotext Geomembr*, 32, pp. 104-110, 2012, <https://doi.org/10.1016/j.geotexmem.2011.11.001>
- Raju, D. M., and R. J. Fannin. "Load-strain-displacement response of geosynthetics in monotonic and cyclic pullout", *Canadian Geotechnical Journal*, 35(2), pp. 183-193, 1998, <https://doi.org/10.1139/t97-088>
- Razzazan, S., A. Keshavarz, and M. Mosallanezhad. "Pullout behavior of polymeric strip in compacted dry granular soil under cyclic tensile load conditions", *J Rock Mech Geotech Eng*, 10(5), pp. 968-976, 2018, <https://doi.org/10.1016/j.jrmge.2018.04.007>
- Viana da Fonseca, A., M. Matos Fernandes, and A. Silva Cardoso. "Interpretation of a footing load test on a saprolitic soil from granite", *Géotechnique*, 47(3), pp. 633-651, 1997, <https://doi.org/10.1680/geot.1997.47.3.633>
- Vieira, C. S., F. B. Ferreira, P. M. Pereira, and M. L. Lopes. "Pullout behaviour of geosynthetics in a recycled construction and demolition material - effects of cyclic loading", *Transp Geotech*, 23, 100346, 2020, <https://doi.org/10.1016/j.trgeo.2020.100346>
- Vieira, C. S., P. M. Pereira, F. B. Ferreira, and M. L. Lopes. "Pullout behaviour of geogrids embedded in a recycled construction and demolition material. Effects of specimen size and displacement rate", *Sustainability*, 12(9), 3825, 2020, <https://doi.org/10.3390/su12093825>
- Watanabe, K., K. Kojima, and A. Kudo. "Influence of cyclic load on pullout stiffness of geogrid embedded in well-graded gravel", *Geosynth Int*, 29(4), pp. 442-456, 2022, <https://doi.org/10.1680/jgein.21.00045>